Ruthenium Complexes

International Edition: DOI: 10.1002/anie.201605687
German Edition: DOI: 10.1002/ange.201605687

From 0 to II in One-Electron Steps: A Series of Ruthenium Complexes Supported by $TropPPh_2$

Xiuxiu Yang, Thomas L. Gianetti, Joshua Harbort, Michael D. Wörle, Lilin Tan, Cheng-Yong Su, Pascal Jurt, Jeffrey R. Harmer,* and Hansjörg Grützmacher**

Abstract: *We report the synthesis of a series of ruthenium complexes supported by the phosphine olefin ligand $tropPPh_2$ (trop = 5-H-dibenzo-[a,d]cyclohepten-5-yl) in the oxidation states 0, +I, and +II, formed via successive one-electron oxidization steps from $Ru^0(tropPPh_2)_2$. The bidentate character of the $tropPPh_2$ ligand and its steric hindrance force the complexes to adopt uncommon geometries, which were investigated by X-ray diffraction analysis. EPR data of the mononuclear Ru^I complex reveal couplings of the unpaired spin with the ruthenium and two phosphorus nuclei, as well as the olefinic protons which show that the spin is mainly localized on the Ru^I center.*

Low valent and/or coordinately unsaturated ruthenium complexes are key intermediates in many ruthenium-catalyzed homogeneous reactions. In 1995, Caulton and coworkers reported the first example of a four-coordinated 16-electron Ru^0 species *cis,trans*-$Ru(CO)_2(PR^1{}_2R^2)_2$ (R^1 = *t*-Bu, R^2 = Me) with butterfly geometry.[1] This geometry is caused by the high energy of ruthenium d-orbitals and the strong back-donation from the electron rich ruthenium center into CO π*-orbitals. That d^8 transition metal complex exhibits a very low activation barrier towards coordination and oxidative addition reactions of CO, O_2, CS_2, C_2H_4, PhC≡CPh, H_2, Cl_2, HCl, or PhC≡CH and can be viewed as a rare model for Ru^0 intermediates in catalytic reactions.[1b]

Our previous work has shown that the bidentate phosphine $tropPPh_2$ in which the Ph_2P group (σ-donor) binds to the concavely shaped 5-H-dibenzo-[a,d]cyclohepten-5-yl (trop) group with an olefin, $C{=}C_{trop}$, as an additional π-accepting binding site[2] coordinates strongly to various transition metal centers, such as palladium,[3a] rhodium,[3b,c] and iridium,[3b,d] and especially stabilizes low-valent oxidation states.

Complexes with ruthenium in a low oxidation state have recently been discovered as catalysts for alkene metathesis reactions, hydrogenation, and dehydrogenation reactions.[4] Generally, complexes with transition metals in the 5th and 6th row undergo reactions such as oxidative addition and reductive elimination in which the oxidation state changes by two units, while complexes with 4th row metals frequently show one-electron redox chemistry.[5] Consequently, Ru^I complexes are rare. Ruthenium complexes with redox active ligands have been reported to undergo one-electron reductions/oxidations, but these occur at the ligand while the oxidation state at the metal center remains +2.[6] Without such ligands, mononuclear Ru^I complexes are inherently unstable.[7] For this reason, most of the Ru^I species are reactive intermediates detected in situ,[7,8] or form binuclear/multinuclear complexes containing metal–metal bonds.[8] To date, the only genuine mononuclear Ru^I complex, reported by Peters et al., is a five-coordinate, 16-electron, trigonal bipyramidal species with 76% of the spin density located at the metal center.[9]

Herein, we report a series of mononuclear ruthenium complexes coordinated only by two $tropPPh_2$ ligands in the oxidation states 0, +1, and +2 (Scheme 1). The metal-containing part in these compounds shows the same chemical composition but has remarkably different structures.

$Ru^0(tropPPh_2)_2$ (**1**) was prepared by heating a mixture of $RuH_2(PPh_3)_4$ and $tropPPh_2$[2] in DME at 80 °C for two days without stirring, during which **1** crystallized out of the solution

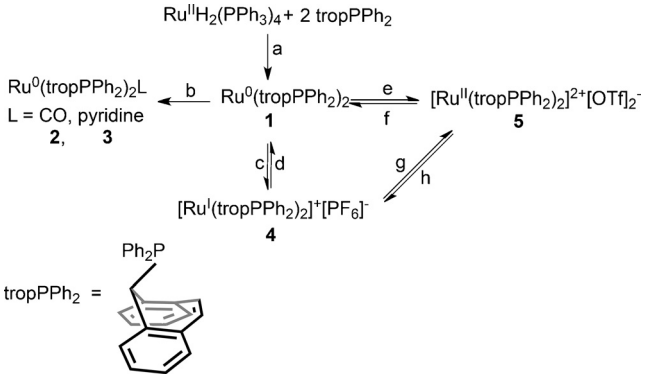

Scheme 1. Synthesis of complexes **1**–**5**. a) DME, 80 °C, 2 days; b) DCM, CO, or pyridine, r.t., < 5 min; c) $[Cp_2Fe][PF_6]$, THF, r.t., overnight; d) $Cr(C_6H_6)_2$, THF, r.t., 7 h; e) AgOTf, THF or DCM, r.t., 2 h; f) $Cp^*{}_2Co$, DME, r.t., 7 h; g) AgOTf, DCM, r.t., 11 h (one anion in **5** is PF_6^-); h) Cp_2Co, THF, r.t., 1 day (anion in **4** is OTf^-).

[*] X. Yang, Dr. T. L. Gianetti, Dr. M. D. Wörle, Dr. L. Tan, P. Jurt, Prof. Dr. H. Grützmacher
Department of Chemistry and Applied Biosciences
Vladimir-Prelog-Weg 1, 8093 Zürich (Switzerland)
E-mail: gianetti@inorg.chem.ethz.ch
hgruetzmacher@ethz.ch
J. Harbort, Assoc. Prof. J. R. Harmer
Center for Advanced Imaging, University of Queensland
St Lucia, Qld, 4072 (Australia)
E-mail: jeffrey.harmer@cai.uq.edu.au
Dr. L. Tan, Prof. Dr. C.-Y. Su, Prof. Dr. H. Grützmacher
Lehn Institute of Functional Materials (LIFM), Sun Yat-Sen University
510275 Guangzhou (China)
Supporting information and the ORCID identification number(s) for the author(s) of this article can be found under: http://dx.doi.org/10.1002/anie.201605687.

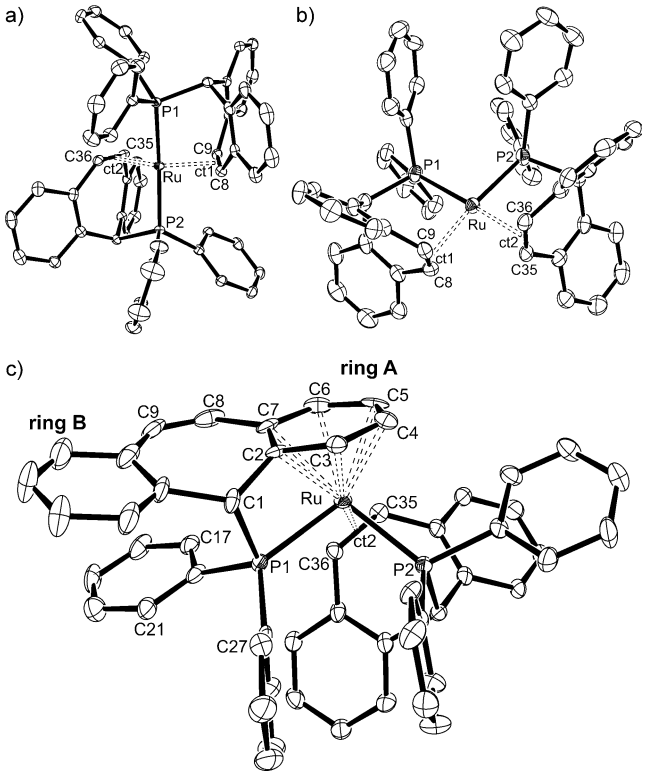

Figure 1. Solid-state structures of a) $Ru^0(tropPPh_2)_2$ (**1**), b) $[Ru^I(tropPPh_2)_2][PF_6]$ (**4**), and c) $[Ru^{II}(tropPPh_2)_2][OTf]_2$ (**5**). Ellipsoids are set at 50% probability; hydrogen atoms, anions, and solvent molecules in the lattice are omitted for clarity. ct is the centroid of the coordinated C8–C9 (in **1** and **4**), C35–C36 bonds, and the coordinated ring A (in **5**), respectively (for more details see the Supporting Information).

in 60% yield (Scheme 1). An X-ray diffraction study of a single crystal of **1** (see the Supporting Information),[10] revealed that the ruthenium center is coordinated to two $tropPPh_2$ ligands in a butterfly coordination environment (Figure 1a). The phosphorus atoms are *trans* to each other, occupying the axial positions and forming a P-Ru-P angle of 173.1°. The P-Ru-olefin angles are nearly at 90°, and the two olefinic moieties occupy the equatorial axis at an angle of 142.3°. Although two phenyl groups on the phosphine ligands point toward the vacant site of the butterfly structure, the shortest Ru–C and Ru–H bonds are 3.38 Å and 2.78 Å, respectively, ruling out the presence of agostic interactions. The IR spectrum of **1** shows no absorptions attributable to Ru–H bonds, supporting the assignment of a four coordinated Ru complex (see the Supporting Information).[11] ^{31}P NMR spectra show one singlet at $\delta = 93.1$ ppm, suggesting that C_2 symmetry is maintained in solution. On the other hand, ^1H NMR analysis shows broad resonance signals at room temperature, and proton exchanges were detected by ^1H–^1H EXSY experiments. This suggests an inversion along the P-Ru-P axis via a planar activated complex at a transition state with $\Delta H^{\neq} = 14.5\ kcal\,mol^{-1}$ and $\Delta S^{\neq} = -4.4\ kcal\,mol^{-1}$ (see the Supporting Information).[12] Aromatic protons show no obvious high field shift (7.39–6.66 ppm), further supporting the lack of agostic interaction between any of the aromatic protons and the metal center.[13]

Addition of one CO or pyridine to **1** yielded five-coordinate complexes **2** or **3** of the type $Ru^0(L)(tropPPh_2)_2$ in high yields (L = CO, pyridine), which were characterized by NMR and IR spectroscopy (see the Supporting Information). These reactions show that the Ru^0 center is Lewis acidic, as was also observed for related d^8 valence electron configured Rh^I and Ir^I $tropPPh_2$ complexes[3b] and Rh^I amido olefin complex, $[Rh(Ntrop_2)(PPh_3)]$, which is an excellent hydrogenation and dehydrogenation catalyst.[12,14]

The cyclic voltammogram (CV) of **1** in dichloromethane solution (see the Supporting Information) shows a quasi-reversible redox wave at −0.30 V and an irreversible oxidation at +0.40 V (vs. ferrocene/ferrocenium; Fc/Fc) which are assigned to $Ru^{I/0}$ and $Ru^{II/I}$ couples, respectively. Chemical oxidation of **1** in THF using one equivalent of $[Cp_2Fe][PF_6]$ or two equivalents of AgOTf produce $[Ru^I(tropPPh_2)_2][PF_6]$ (**4**) and $[Ru^{II}(tropPPh_2)_2][OTf]_2$ (**5**), respectively. Crystals of **4** suitable for X-ray diffraction were grown by slow diffusion of a DME/hexane mixture into a saturated THF solution of **4** (see the Supporting Information).[10] The solid-state structure of the $[Ru^I(tropPPh_2)_2]^+$ cation is the first of an unsaturated 15-electron mononuclear Ru^I complex and reveals a slightly distorted planar geometry. The two P atoms are *cis* to each other and the two olefin bonds deviate out of the plane defined by P-Ru-P (Figure 1b). The coordinating $C{=}C_{trop}$ bonds (that is, of C8–C9 and C35–C36) are 0.06 Å longer than in the free ligand,[2] but 0.05 Å shorter than **1** which reflects the slightly smaller back-donation of electron density from the Ru^I center to the π*-orbitals of the olefins in **4** as compared to **1**.

The electronic structure of **4** was characterized by field-sweep EPR and HYSCORE spectroscopy. The principal g-values and Ru hyperfine couplings (Table 1) were determined from field-sweep EPR spectra at X-band (9.735 GHz; Sup-

Table 1: EPR parameters for Complex **4**.[a]

Interaction	Principal values / error[e]	Spin population
g-value	1.9745, 2.405, 2.445 / ±0.0005 (2.0087, 2.3921, 2.4395)	NA
^{101}Ru[b]	−165, ≤−145,[c] ≤−145[c] / ±5 (−229, −153, −151)	1.0–1.2[d] (1.17)
^{31}P	−28, −29, −36 / ±0.5 (−28.7, −29.5, −36.3) (−28.4, −29.2, −36.0)	−0.026–−0.038 (−0.036) (−0.036)
$^1H_{olf1}$	[−3.5, −4.0, 7.5] −0.5 / ±0.5 ([−2.5, −4.0, 6.6] −0.2)	<0.003 (0.000)
$^1H_{olf2}$	[−5.0, −4.0, 9.0] + 2.0 / ±0.5 ([−2.8, −3.9, 6.7] + 1.5)	<0.003 (0.002)

[a] DFT values are in parentheses. Hyperfine couplings are in MHz; the sign of the experimental hyperfine values were assigned according to the DFT. An extended version including principal value orientations and DFT atomic coordinates is given in the Supporting Information, Tables S2, S3. [b] $^{99,101}Ru$, $I = 5/2$, abundance 12.76%, 17.06%. [c] Values estimated from the low field shoulder of the X-band EPR spectrum. [d] Range estimated using Equation (1) and the DFT distances. [e] Error estimate for each principal value.

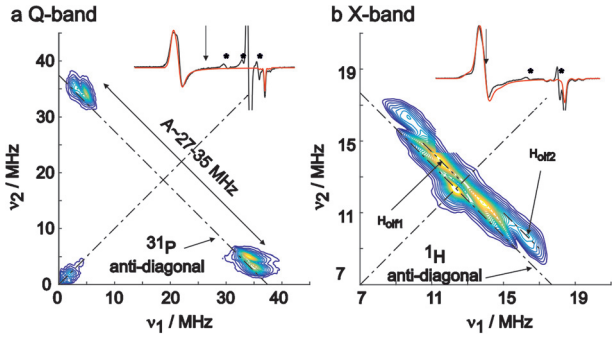

Figure 2. Representative HYSCORE spectra at a) Q-band and b) X-band showing couplings from two ^{31}P nuclei and the closest olefinic protons, respectively. Insets: FID-detected EPR spectra used to obtain the g-values and Ru hyperfine couplings; experiment (black), simulation (red). The vertical line marks the field position of the HYSCORE measurement, and ⋆ marks features from decay product and background resonator signals.

porting Information, Figure S1)/ Q-band (34.21 GHz, Figure S2) as shown in the insets of Figure 2 a,b. ^{31}P and ^{1}H hyperfine couplings, which are not resolved in the field-sweep EPR spectra, were measured by HYSCORE at Q-band and X-band, respectively. Figure 2 a shows a spectrum recorded near g_2/g_3 that exhibits cross-peaks from the two ^{31}P nuclei with a hyperfine coupling of $A = 28$–36 MHz. HYSCORE spectra recorded at a set of field positions across the EPR spectrum (Supporting Information, Figure S3) and their simulation allowed the three ^{31}P principal hyperfine values to be extracted. The X-band HYSCORE data in Figure 2 b (Supporting Information, Figure S4) allowed the largest ^{1}H dipolar couplings to be determined, as cross-peaks are shifted behind the anti-diagonal line at the ^{1}H Larmor frequency according to the magnitude of the dipolar coupling (pseudo-secular part of the hyperfine interaction). The simulation of the HYSCORE spectra allowed two proton hyperfine couplings to be determined that we assign to the protons closest to the Ru ion; two sets of essentially magnetically equivalent olefinic protons both with $r(\mathrm{Ru{-}H_{olf}}) = 2.8$ Å (distance from DFT geometry). The anisotropic part of the hyperfine interactions of H_{olf1} and H_{olf2} enables an estimate of the spin population ρ on the Ru ion using the point-dipolar formula:

$$\mathbf{T} = \frac{\mu_0}{4\pi\hbar} g_e \mu_B g_n \mu_N \sum_i \rho_i \frac{3\,\mathbf{n}_i \mathbf{n}_i^{\mathrm{T}} - 1}{r_i^{\,3}} \qquad (1)$$

where $\mathbf{T}$ is the anisotropic part of the hyperfine coupling and $\mathbf{n}_i$ is the (spin population—nuclear spin) unit vector with r the corresponding distance. With r_{olf}/ $r_{P1,P2} = 2.8/4.1,4.9$ Å, the Ru spin population is computed as $\rho(\mathrm{Ru}) = 1.0$–1.2 (see the Supporting Information). Further interpretation of the experimental EPR data was aided by density functional theory (DFT) calculations, a summary of which is given in Table 1 (values in parentheses). As can be seen, the principal g-values and hyperfine couplings from ^{101}Ru, ^{31}P, and the olefinic protons are well modeled by the calculation. From the DFT results, the ^{31}P hyperfine interaction and spin population is negative (ρ(p-type) $= -0.029$) and thus due to polarization from the SOMO, which is largely comprised of Ru orbitals (ρ(s-type) $= 0.17$, ρ(p-type) $= 0.04$, and ρ(d-type) $= 0.96$). The DFT spin population distribution leads to two sets of olefinic proton hyperfine couplings, as is observed experimentally, with DFT predicting $\rho = -0.047$ on each olefinic moiety (see the Supporting Information). Both experimental and computational data firmly establish the electronic structure of **4** as a valence-localized Ru$^{\mathrm{I}}$ ion.

Oxidizing **1** with two equivalents of AgOTf ($E^{\circ\prime} = 0.65$ V[15]) in DCM at room temperature produced **5** in 93 % yield after extraction by DME. ^{19}F NMR shows a typical singlet signal of free OTf^- in solution, while in the ^{31}P NMR spectrum two doublets were observed at 93.3 and −85.1 ppm suggesting two chemically inequivalent phosphorus atoms. Moreover, the J_{PP} coupling constant of 35 Hz implies that the two phosphorus nuclei are in *cis* position. The unusually low frequency shift of one phosphorus (P1) indicates an uncommon coordination pattern.

Single crystals of **5** were grown from a 1,4-dioxane solution at room temperature (see the Supporting Information).[10] A structural view of **5** is depicted in Figure 1 c. Indeed, one tropPPh$_2$ ligand is bound to the metal center by the phosphorus atom and one of the arene rings (Figure 1 c, ring A) of the trop moiety, while the C8=C9 unit is unbound. The second ligand coordinates via the phosphorus atom and the olefinic moiety C35=C36, which is 0.6 Å longer than the C8=C9. In this coordination sphere the Ru$^{\mathrm{II}}$ center attains a valence electron count of 18.[16] Coordination of the arene rings causes considerably distortion within the corresponding tropPPh$_2$ ligand: The 5-H-dibenzo-[a,d]cyclohepten-5-yl unit is flattened and the angle between ring A and ring B is only 22.6°, while in the second trop ligand this angle is 60.2° (49.5° in free tropPPh$_2$).[2] Also the Ru-P1-C1 angle is rather acute (89.53°), while the corresponding angle in the normally bound tropPPh$_2$ is 111.28°. In the ^{31}P NMR spectrum we assign the chemical shift at $\delta = 93.3$ ppm to P2 which is typical and indicative for the classic binding mode of the tropPPh$_2$ ligand. The shift at $\delta = -85.1$ ppm for P1 may be the result of the particular binding mode and distortion within the κ(P),η^6-bound ligand.[17] In the ^{13}C NMR spectrum in $CDCl_3$, four resonances at distinctively lower frequencies (89.4–119 ppm) are assigned to the coordinated carbon nuclei C3, C4, C5, and C7. The same holds for the coordinated C35=C36 bond, which shows signals at $\delta = 72.6$, 78.2 ppm at significantly lower frequency than the non-coordinated C8=C9 unit ($\delta = 131$, 143.2 ppm). The NMR data clearly indicate that **5** retains the same structure in solution as in the solid state. As shown in Scheme 1, the redox reactions are fully reversible and the dication **5** can be reduced with cobaltocene, $CoCp_2$, back to the radical cation **4**, which in turn reacts with decamethylcobatocene, $CoCp^*_2$, to the neutral Ru^0 complex **1**.

In conclusion, we have synthesized Ru^0(tropPPh$_2$)$_2$ (**1**), another but yet rare example of a d^8-Ru^0 complex with a butterfly structure. Based on the CV potentials of **1**, complexes with d^7-Ru$^{\mathrm{I}}$ and d^6-Ru$^{\mathrm{II}}$ centers have been chemically prepared and were fully characterized. These data confirms that ruthenium can undergo one-electron redox reactions at the metal center and each individual oxidation state is sufficiently stabilized by the tropPPh$_2$ ligand to allow

isolation. EPR analysis firmly establishes **4** as a radical with the unpaired electron spin mainly localized on the Ru center which is in contrast to the neutral d^9-valence electron configured Rh^0 complexes which have a comparable composition but are best described as delocalized organometallic radicals.[18]

Acknowledgements

This work was financed by the Swiss National Science Foundation (grant 200021 162437/1) and the ETH Zürich (grant 2-77230-15). X.Y. is grateful for financial support from the China Scholarship Council, T.L.G. from ETH Zürich Postdoctoral Fellowship Program (FEL-14 15-1), and J.R.H. from the ARC (FT120100421) and the Australian National Fabrication Facility for use of equipment. We thank Prof. Dr. Paul S. Pregosin for the helpful discussions on the NMR data of complex **5**. Dr. Reinhard Kissner and Dr. Daniel Klose (EPR), Dr. Xiangyang Zhang (HRMS), and Dr. Xiaodan Chen (XRD) are gratefully acknowledged for measurements.

Keywords: metal radicals · non-redox ligands · one-electron oxidation · P ligands · ruthenium

How to cite: *Angew. Chem. Int. Ed.* **2016**, *55*, 11999–12002
Angew. Chem. **2016**, *128*, 12178–12181

[1] a) M. Ogasawara, S. A. Macgregor, W. E. Streib, K. Folting, O. Eisenstein, K. G. Caulton, *J. Am. Chem. Soc.* **1995**, *117*, 8869–8870; b) M. Ogasawara, S. A. Macgregor, W. E. Streib, K. Folting, O. Eisenstein, K. G. Caulton, *J. Am. Chem. Soc.* **1996**, *118*, 10189–10199; c) M. Ogasawara, D. Huang, W. E. Streib, J. C. Huffman, N. Gallego-Planas, F. Maseras, O. Eisenstein, K. G. Caulton, *J. Am. Chem. Soc.* **1997**, *119*, 8642–8651; d) R. Flügel, B. Windmüller, O. Gevert, H. Werner, *Chem. Ber.* **1996**, *129*, 1007–1013.

[2] tropPPh$_2$ ligand: J. Thomaier, S. Boulmaâz, H. Schönberg, H. Rüegger, A. Currao, H. Grützmacher, H. Hillebrecht, H. Pritzkow, *New J. Chem.* **1998**, *22*, 947–958.

[3] a) L. Bettucci, C. Bianchini, W. Oberhauser, M. Vogt, H. Grützmacher, *Dalton Trans.* **2010**, *39*, 6509–6517; b) F. Breher, H. Rüegger, M. Mlakar, M. Rudolph, S. Deblon, H. Schönberg, S. Boulmaâz, J. Thomaier, H. Grützmacher, *Chem. Eur. J.* **2004**, *10*, 641–653; c) H. Schönberg, S. Boulmaâz, M. Wörle, L. Liesum, A. Schweiger, H. Grützmacher, *Angew. Chem. Int. Ed.* **1998**, *37*, 1423–1426; *Angew. Chem.* **1998**, *110*, 1492–1494; d) S. Boulmaâz, M. Mlakar, S. Loss, H. Schönberg, S. Deblon, M. Wörle, R. Nesper, H. Grützmacher, *Chem. Commun.* **1998**, 2623–2624.

[4] a) G. C. Vougioukalakis, R. H. Grubbs, *Chem. Rev.* **2010**, *110*, 1746–1787; b) C. Gunanathan, D. Milstein, *Chem. Rev.* **2014**, *114*, 12024–12087; c) R. Noyori, T. Ohkuma, *Angew. Chem. Int. Ed.* **2001**, *40*, 40–73; *Angew. Chem.* **2001**, *113*, 40–75; d) R. E. Rodríguez-Lugo, M. Trincado, M. Vogt, F. Tewes, G. Santiso-Quinones, H. Grützmacher, *Nat. Chem.* **2013**, *5*, 342–347.

[5] P. J. Chirik, K. Wieghardt, *Science* **2010**, *327*, 794–795.

[6] Recent examples of ruthenium complexes coordinated by redox ligands: a) P. Mondal, A. Das, G. K. Lahiri, *Inorg. Chem.* **2016**, *55*, 1208–1218; b) G. Skara, M. Gimferrer, F. D. Proft, P. Salvador, B. Pinter, *Inorg. Chem.* **2016**, *55*, 2185–2199; c) P. Ghosh, S. Mandal, I. Chatterjee, T. K. Mondal, S. Goswami, *Inorg. Chem.* **2015**, *54*, 6235–6244.

[7] Ru^I: a) Q. G. Mulazzani, S. Emmi, P. G. Fuochi, M. Z. Hoffman, M. Venturi, *J. Am. Chem. Soc.* **1978**, *100*, 981–983; b) M. Schröder, T. A. Stephenson, G. Wilkinson, R. D. Gillard, J. A. McCleverty, *Comprehensive Coordinarion Chemistry*, *Vol. IV*. Pergamon, New York, **1987**, p. 277; c) C. Bianchini, M. Peruzzini, A. Ceccanti, F. Laschi, P. Zanello, *Inorg. Chim. Acta* **1997**, *259*, 61–70; d) R. J. Angelici, B. Zhu, S. Fedi, F. Laschi, P. Zanello, *Inorg. Chem.* **2007**, *46*, 10901–10905; e) M. K. Biswas, S. C. Patra, A. N. Maity, S. Ke, N. D. Adhikary, P. Ghosh, *Inorg. Chem.* **2012**, *51*, 6687–6699; f) C. Bianchini, F. Laschi, M. Peruzzini, P. Zanello, *Gazz. Chim. Ital.* **1994**, *124*, 271–274.

[8] E. A. Seddon, K. R. Seddon in *The chemistry of ruthenium*, Elsevier, Amsterdam, **1984**, pp. 891–925.

[9] a) A. Takaoka, L. C. H. Gerber, J. C. Peters, *Angew. Chem. Int. Ed.* **2010**, *49*, 4088–4091; *Angew. Chem.* **2010**, *122*, 4182–4185; b) A. Takaoka, M.-E. Moret, J. C. Peters, *J. Am. Chem. Soc.* **2012**, *134*, 6695–6706.

[10] a) CCDC 1468782 (**1**), 1456317 (**4**), and 1468803 (**5**) contain the supplementary crystallographic data for this paper. These data can be obtained free of charge from The Cambridge Crystallographic Data Centre; b) L. J. Bourhis, O. V. Dolomanov, R. J. Gildea, J. A. K. Howard, H. Puschman, *Acta Crystallogr. Sect. A* **2015**, *71*, 59–75; c) O. V. Dolomanov, L. J. Bourhis, R. J. Gildea, J. A. K. Howard, H. Puschman, *J. Appl. Crystallogr.* **2009**, *42*, 339–341.

[11] J. P. Lee, Z. Ke, M. A. Ramírez, T. B. Gunnoe, T. R. Cundari, P. D. Boyle, J. L. Petersen, *Organometallics* **2009**, *28*, 1758–1775.

[12] P. Maire, T. Büttner, F. Breher, P. Le Floch, H. Grützmacher, *Angew. Chem. Int. Ed.* **2005**, *44*, 6318–6323; *Angew. Chem.* **2005**, *117*, 6477–6481.

[13] For the C–H agostic bond with ruthenium see: a) J. Mathew, N. Koga, C. H. Suresh, *Organometallics* **2008**, *27*, 4666–4670; b) S. Burling, E. Mas-Marzà, J. E. V. Valpuesta, M. F. Mahon, M. K. Whittlesey, *Organometallics* **2009**, *28*, 6676–6686.

[14] T. Zweifel, J.-V. Naubron, H. Grützmacher, *Angew. Chem. Int. Ed.* **2009**, *48*, 559–563; *Angew. Chem.* **2009**, *121*, 567–571.

[15] N. G. Connelly, W. E. Geiger, *Chem. Rev.* **1996**, *96*, 877–910.

[16] S. H. Hong, A. Chlenov, M. W. Day, R. H. Grubbs, *Angew. Chem. Int. Ed.* **2007**, *46*, 5148–5151; *Angew. Chem.* **2007**, *119*, 5240–5243.

[17] For ^{31}P NMR low frequency shifts, see: a) P. S. Pregosin, *NMR in organometallic chemistry*, Wiley-VCH, Weinheim, **2012**; b) O. Kühl, *Phosphorus-31 NMR Spectroscopy*, Springer, Berlin, **2008**; c) A. Cassen, L. Vendier, J. Daran, A. I. Poblador-Bahamonde, E. Clot, G. Alcaraz, S. Sabo-Etienne, *Organometallics* **2014**, *33*, 7157–7163; d) H. Caldwell, S. Isseponi, P. S. Pregosin, A. Albinati, S. Rizzato, *J. Organomet. Chem.* **2007**, *692*, 4043–4051.

[18] B. de Bruin, J. C. Russcher, H. Grützmacher, *J. Organomet. Chem.* **2007**, *692*, 3167.

Received: June 12, 2016
Published online: August 25, 2016

